

Lawrence Berkeley National Laboratory

Lawrence Berkeley National Laboratory

Title

CANCELLED Molecular dynamics simulations of noble gases in liquid water: Solvati on structure, self-diffusion, and kinetic isotope effect

Permalink

<https://escholarship.org/uc/item/10n4s6jz>

Authors

Bourg, I.C.
Sposito, G.

Publication Date

2008-06-03

Peer reviewed

1 **Molecular dynamics simulations of noble gases in liquid water: Solvation structure, self-**
2 **diffusion, and kinetic isotope effect**

3

4 Ian C. Bourg^{1*}, Garrison Sposito¹

5

6 ¹ Geochemistry Department, Earth Sciences Division, Lawrence Berkeley National Laboratory,
7 Berkeley, CA 94720, USA

8

9

10

11 Both authors contributed equally to research design, data analysis and manuscript writing. The
12 lead author carried out the molecular dynamics simulations.

13

14 Classification: Physical Sciences; Geophysics.

15

16

17 *Author to whom correspondence should be addressed (ibourg@nature.berkeley.edu)

18

19

20 **Abstract**

21
22 Despite their great importance in low-temperature geochemistry, self-diffusion coefficients of
23 noble gas isotopes in liquid water (D) have been measured only for the major isotopes of helium,
24 neon, krypton and xenon. Data on the self-diffusion coefficients of minor noble gas isotopes are
25 essentially non-existent and so typically are estimated by a kinetic theory model in which D
26 varies as the inverse square root of the isotopic mass (m): $D \propto m^{-0.5}$. To examine the validity of
27 the kinetic theory model, we performed molecular dynamics (MD) simulations of the diffusion
28 of noble gases in ambient liquid water with an accurate set of noble gas-water interaction
29 potentials. Our simulation results agree with available experimental data on the solvation
30 structure and self-diffusion coefficients of the major noble gas isotopes in liquid water and reveal
31 for the first time that the isotopic mass-dependence of all noble gas self-diffusion coefficients has
32 the power-law form $D \propto m^{-\beta}$ with $0 < \beta < 0.2$. Thus our results call into serious question the
33 widespread assumption that the ‘square root’ model can be applied to estimate the kinetic
34 fractionation of noble gas isotopes caused by diffusion in ambient liquid water.

35 **Introduction**

36 Dissolved noble gases have proven to be important geochemical indicators of transport
37 processes and paleoclimate in hydrogeological basins (1-7), lacustrine sediments (8-10),
38 aquitards (11-13), engineered clay barriers (14) and the oceans (15). Brennwald et al. (10) used
39 Ne, Ar, Kr and Xe concentrations and $^{20}\text{Ne}/^{22}\text{Ne}$ and $^{36}\text{Ar}/^{40}\text{Ar}$ isotopic ratios to estimate rates of
40 methane release from anoxic lake sediments. Rübél et al. (12) used ^4He concentrations and
41 $^{40}\text{Ar}/^{36}\text{Ar}$ isotopic ratios to evaluate the relative importance of advective and diffusive transport
42 in a clay-rich geological formation proposed to become host to a Swiss high-level radioactive
43 waste repository. Stute et al. (1) used Ne, Ar, Kr and Xe concentrations in a Brazilian aquifer to
44 reconstruct continental temperatures during the last 30,000 years. In the paleotemperature
45 reconstruction method of Stute et al. (1), noble gas concentrations in aquifer water were assumed
46 to result from three successive steps: equilibrium dissolution of noble gases at the phreatic
47 surface at the time of groundwater recharge, uptake of excess noble gas through complete
48 dissolution of trapped atmospheric air near the water table, and diffusion-controlled release of a
49 fraction of the excess noble gas (1, 3). For each noble gas other than Ne, the mass fraction
50 released during the third step ($1-f_{NG}$) is related to the mass fraction of neon released during the
51 third step ($1-f_{\text{Ne}}$) by the well-known Rayleigh fractionation formula (if D_{NG} is the self-diffusion
52 coefficient of a noble gas in water):

$$53 \quad f_{NG} = f_{\text{Ne}}^{D_{NG}/D_{\text{Ne}}} \quad [1]$$

54 Pore water concentrations of the four noble gases Ne, Ar, Kr and Xe then allow the calculation
55 of the four unknown parameter-values: ground temperature and atmospheric pressure at the time
56 and location of groundwater recharge, total amount of dissolved 'excess air', and f_{Ne} (1, 3).

57 Paleotemperatures calculated in this way are most sensitive to Xe concentrations, because the
58 temperature-dependence of noble gas solubility increases with atomic mass (3).

59 Despite the importance of noble gas diffusion coefficients in low-temperature geochemistry,
60 remarkably few measurements of these critical parameters have been reported. Jähne et al. (16)
61 measured self-diffusion coefficients of four noble gases in liquid water at 298 K (Table 1).
62 Pulsed field gradient nuclear magnetic resonance (PFG NMR) studies (17, 18) confirmed the
63 result of Jähne et al. (16) for Ne diffusion, but yielded a significantly larger Xe self-diffusion
64 coefficient (18). No other experimental data on noble gas diffusion in liquid water appear to have
65 been published during the last twenty years. Data on the self-diffusion coefficients of minor
66 noble gas isotopes are even more scarce: they consist of a single measurement of the ratio of the
67 self-diffusion coefficients of ^3He and ^4He : $D(^3\text{He})/D(^4\text{He}) = 1.15 \pm 0.03$ (16).

68 With this extreme paucity of experimental data, most geochemical studies of noble gas
69 solutes have relied upon the He, Ne, Kr and Xe diffusion coefficients measured by Jähne et al.
70 (16) together with Ar diffusion coefficients estimated by extrapolation of the results of Jähne et
71 al. (16) (1, 3-6, 8-13, 15, 19). Self-diffusion coefficients of minor noble gas isotopes in liquid
72 water for which no data exist then have routinely been estimated using the kinetic-theory model
73 $D \propto 1/\mu^{0.5}$ [μ is the solvent-solute reduced mass, $\mu = mm_0/(m + m_0)$, if m and m_0 are solute and
74 solvent molecular masses (7)] or, more commonly, the relation $D \propto 1/m^{0.5}$, which is obtained
75 from the kinetic-theory model under the assumption that the hydrogen-bonded water network
76 behaves as an ‘effective particle’ of infinitely large mass ($m_0 \gg m$) (4, 6, 9, 10, 19). Use of the
77 relation $D \propto 1/m^{0.5}$ in conjunction with measured $^{20}\text{Ne}/^{22}\text{Ne}$ or $^{36}\text{Ar}/^{40}\text{Ar}$ solute isotopic ratios in
78 porous media has led to a widespread dismissal of diffusion in pore water as a significant

79 contributor to noble gas transport (4, 6, 10, 19) and, in particular, to strong dismissal (4, 19) of
80 the paleotemperature reconstruction method developed by Stute et al. (1).

81 Very recently Richter et al. (20) discovered somewhat unexpectedly that the self-diffusion
82 coefficients of ionic solutes in liquid water do not follow the ‘square-root’ model in their
83 dependence on isotopic mass. They provided the first precise measurements of the kinetic
84 fractionation of Mg, Li, and Cl isotopes by diffusion in liquid water and showed that a more
85 general inverse power-law relation, $D \propto m^{-\beta}$, was applicable, with $\beta_{\text{Mg}} \sim 0$, $\beta_{\text{Li}} = 0.0148 \pm 0.0017$
86 and $\beta_{\text{Cl}} = 0.026 \pm 0.014$. Our subsequent molecular dynamics (MD) simulations of the self-
87 diffusion of these ions (21) fully corroborated the small experimental β -values and provided
88 insight based on hydration shell dynamics as to why β differed among the three ions.

89 The very low solubility of noble gases in ambient water currently prevents the use of the
90 experimental method of Richter et al. (20) to measure the mass-dependence of their self-
91 diffusion coefficients (F. M. Richter, personal communication, 2006). The self-diffusion
92 coefficients of noble gas isotopes in liquid water can be calculated, however, by MD simulation.
93 The accuracy of simulations performed for this purpose is limited mainly by the quality of the
94 water-water and noble gas-water intermolecular potentials used. Previous molecular simulations
95 of noble gas solutes in ambient water (22-29) have incorporated noble gas-water potentials
96 calculated either from somewhat outdated noble gas-noble gas interaction data (30) or with
97 approximate (Lorentz-Berthelot) combining rules. Noble gas-water potentials used in these
98 studies were tested only by comparing model predictions with experimental data on the enthalpy
99 and Gibbs energy of hydration. Gibbs energies of noble gas solvation in ambient water were
100 predicted with about 4 kJ mol⁻¹ inaccuracy; however, the Gibbs energies of solvation of Ne and

101 Xe differ by only 4.3 kJ mol⁻¹ (28). The simulated noble gas self-diffusion coefficients (29) in
102 fact overestimated most experimental data (Table 1).

103 In the present study, MD simulations of noble gas solutes in liquid water were carried out
104 with a new set of noble gas-water potentials calculated with noble gas-noble gas interaction data
105 (31, 32) that are more recent than those of Hirschfelder et al. (30) and with combining rules that
106 are more accurate than the Lorentz-Berthelot rules (33). Our results for the major noble gas
107 isotopes (⁴He, ²⁰Ne, ⁴⁰Ar, ⁸⁴Kr, ¹³²Xe) corroborate available data on their solvation structure (34,
108 35) and self-diffusion coefficients in ambient water (16, 17). Simulations following the
109 methodology of Bourg and Sposito (21) also were performed to determine the isotopic mass-
110 dependence of noble gas self-diffusion coefficients.

111

112 **Solvation structure**

113 The solvation structure near ⁴He, ²⁰Ne, ⁴⁰Ar, ⁸⁴Kr and ¹³²Xe in ambient liquid water as revealed by
114 radial distribution functions is summarized in Figure 1 [radial distribution functions for O and H
115 atoms near noble gas solutes, $g_{NGO}(r)$ and $g_{NGH}(r)$] and Table 2 [location of the first maximum
116 (r_{max}) and minimum (r_{min}) of each $g_{NGO}(r)$ function, and average number of water molecules in the
117 first solvation shell (N_{shell})]. The slightly shorter first-shell peak distance in $g_{NGH}(r)$ as compared
118 to $g_{NGO}(r)$ indicates that first-shell water molecules are preferentially oriented in a “straddling”
119 configuration, such that one of the apices of the water tetrahedron points away from the noble
120 gas atom (36, 37) (Figure 2). This preferred configuration, however, does not require the
121 existence of a static clathrate cage: it exists even for small hydrophobic solutes (H, He, Ne) that
122 diffuse much more rapidly than nearby water molecules and have a ‘floppy’ solvation shell (38).
123 Radial distribution functions for the smallest noble gas atoms, He and Ne, (Figure 1) are similar

124 to those obtained by Kirchner et al. (38) by *ab initio* MD simulation of a solvated uncharged H
125 atom. The evident absence of solvation structure beyond the first shell is consistent with previous
126 MD simulation studies (23, 25).

127 No experimental data appear to be available concerning the solvation structure around noble
128 gases in ambient liquid water. Bowron et al. (35) used extended X-ray absorption fine-structure
129 (EXAFS) spectroscopy to determine the radial distribution function of O atoms around Kr in
130 water at 20 bar and 277 to 348 K. If the results of Bowron et al. (35) are extrapolated to ambient
131 pressure, based on the lack of pressure-dependence of Kr solvation structure in water between 20
132 to 700 bar (39, 40), they are in good agreement with our MD simulation results (data not shown).
133 Broadbent and Neilson (34) calculated the total distribution function of argon [$G_{\text{Ar}}(r)$] in D₂O at
134 298 K and ~240 bar from isotopic-difference neutron diffraction data on natural Ar (^{Nat}Ar) and
135 ³⁶Ar aqueous solutions. The total distribution function is related to the partial radial distribution
136 functions by:

$$137 \quad G_{\text{Ar}}(r) = A[g_{\text{NGO}}(r) - 1] + B[g_{\text{NGH}}(r) - 1] + C[g_{\text{ArAr}}(r) - 1] \quad [2]$$

138 where the weighting coefficients have the values $A = 1.247$, $B = 2.869$ and $C \approx 0$ at 240 bar (34).

139 Our MD simulation of G_{Ar} based on the partial radial distribution functions is also consistent
140 with the experimental G_{Ar} (data not shown).

141

142 **Self-diffusion coefficients**

143 Experimental and simulation results on the self-diffusion coefficients of major noble gas isotopes
144 in water at 298 K are shown in Table 1 and Figure 3. The self-diffusion coefficients predicted in
145 the present study are consistent with the experimental data of Jähne et al. (16). Notably, our Xe
146 simulation results support the experimental results of Jähne et al. (16), not those of Weingärtner

147 et al. (18). Our Ar simulation results also are consistent with D_{Ar} values estimated by
148 extrapolation of the He, Ne, Kr and Xe diffusion data of Jähne et al. (16) [$D_{\text{Ar}} = 2.66 \times 10^{-9} \text{ m}^2 \text{ s}^{-1}$
149 at 298 K (4)].

150

151 **Kinetic fractionation by diffusion in liquid water**

152 The mass dependencies of the self-diffusion coefficients of noble gas isotopes as obtained by
153 MD simulation were analyzed by plotting average $\log D$ values obtained during four 2 ns
154 ‘blocks’ of each 8 ns simulation vs. $\log m$. Linear regression of the data shows that the isotopic
155 mass-dependence of noble gas self-diffusion coefficients has the generic power-law form:

$$156 \quad D \propto m^{-\beta} \quad [3]$$

157 with $\beta > 0$, as proposed originally for ionic solutes by Richter et al. (20) (Linear regression of
158 simulation results as $\log D$ vs. $\log \mu$ yielded a poorer fit than equation 3 for He, Ne, Ar and Xe).

159 The linear regression parameters obtained with equation 3 (Table 3) indicate that $\beta < 0.2$, in
160 stunning contradiction with the kinetic theory model $D \propto 1/m^{0.5}$ (4, 6, 9, 10, 19). For ‘Brownian’
161 particles (i.e., solutes that are much larger and heavier than the solvent molecules), the well-

162 known Stokes-Einstein relation predicts that the self-diffusion coefficient should be independent
163 of isotopic mass (i.e., $\beta = 0$ in equation 3). The decrease in β -values in the order $\text{He} \geq \text{Ne} > \text{Ar} \geq$

164 Xe that we observed suggests that the larger noble gas solutes indeed behave in a more

165 ‘Brownian’ manner than do the smaller noble gas solutes. If the solute radius r (Å) is estimated
166 as r_{max} for g_{NGO} (Table 2) minus half of r_{max} for the O-O radial distribution function in pure water

167 (1.4 Å), then our β -values are well described by the power-law relation $\beta = B (1/r)^\gamma$ with $B = 0.55$
168 ± 0.17 and $\gamma = 2.49 \pm 0.45$ ($R^2 = 0.98$).

169

170 **Conclusions**

171 A new set of noble-gas water interaction parameters, derived with improved combining rules
172 and noble gas-noble gas interaction parameters, allowed successful prediction of all available
173 experimental data on the solvation structure and self-diffusion coefficients of major noble gas
174 isotopes in ambient liquid water. In particular, our simulation results corroborate the self-
175 diffusion coefficients of major noble gas isotopes measured by Jähne et al. (16) that are widely
176 used in geochemical studies (1, 3-6, 8-13, 15, 19). Our MD simulations carried out with a broad
177 range of solute isotopic masses revealed that noble gas self-diffusion coefficients in water follow
178 an inverse power-law mass-dependence, $D \propto m^{-\beta}$, with $0 < \beta < 0.2$. Thus, the commonly invoked
179 ‘square root’ model of noble gas isotope fractionation by diffusion in liquid water (4, 6, 9, 10,
180 19) overestimates the strength of the mass-dependence of noble gas self-diffusion coefficients.

181

182 **Simulation methods**

183 Molecular dynamics simulations (8 ns interval, preceded by 202 ps of equilibration at 298 K)
184 were carried out with the program MOLDY 3.6 (41) for one noble gas atom and 550 water
185 molecules in a periodically replicated, cubic cell (microcanonical ensemble, 0.997 kg dm^{-3}
186 density) with the methodology of Bourg and Sposito (21). Molecular trajectories were calculated
187 by solving the Newton-Euler equations (with a 1 fs time step) with a form of the Beeman
188 algorithm, the most accurate of all “Verlet-equivalent” algorithms (41). Long-range interactions
189 were treated by Ewald summation with parameters chosen to yield an Ewald sum accuracy of
190 99.99%. Total energy drift during each 8 ns simulation was about 0.002 %. Liquid water was
191 described with the extended simple point charge (SPC/E) model of Berendsen et al. (42). Despite
192 its simplicity [fixed O-H bond lengths (1 \AA), H-O-H angle (109.47°) and atomic charges ($q_{\text{O}} = -$

193 0.8476 e and $q_H = 0.4238$ e] the SPC/E model predicts the self-diffusion coefficient of water at
 194 298 K to within 4 ± 17 % (43), the static dielectric constant of water at 324.2 and 523 K (at 1 kg
 195 dm^{-3} density) to within 2 ± 20 and 4 ± 8 % (44), and the X-ray scattering intensities of liquid
 196 water at 298 and 350 K to within 1.8 % (45).

197 On the SPC/E model, short-range non-Coulombic interactions (ϕ_{ij} , kJ mol^{-1}) between water O
 198 atoms are described with the Lennard-Jones (LJ) 6-12 model:

$$199 \quad \phi_{ij}(r_{ij}) = 4 \epsilon_{ij} \left[\left(\frac{\sigma_{ij}}{r_{ij}} \right)^6 - \left(\frac{\sigma_{ij}}{r_{ij}} \right)^{12} \right] \quad [3]$$

200 where r_{ij} (\AA) is the interatomic distance and $2^{1/6}\sigma_{ij}$ and ϵ_{ij} are the location (\AA) and depth of the
 201 potential well (J mol^{-1}). The LJ 6-12 model, with noble gas σ_{ii} and ϵ_{ii} parameters compiled by
 202 Aziz (31), accurately describes interactions between noble gas atoms in the region of the
 203 potential well (32). In the present study, σ_{ij} and ϵ_{ij} parameters for the interaction between noble
 204 gases and water O atoms were calculated from noble gas and SPC/E water σ_{ii} and ϵ_{ii} parameters
 205 with the combining rules of Kong (33):

$$206 \quad \epsilon_{ij} \sigma_{ij}^6 = \sqrt{\epsilon_{ii} \sigma_{ii}^6 \cdot \epsilon_{jj} \sigma_{jj}^6} \quad [4a]$$

$$207 \quad \epsilon_{ij} \sigma_{ij}^{12} = \left[\frac{(\epsilon_{ii} \sigma_{ii}^{12})^{1/13} + (\epsilon_{jj} \sigma_{jj}^{12})^{1/13}}{2} \right]^{13} \quad [4b]$$

208 Equations 4a,b, combined with the kinetic theory of gases, predict self-diffusion coefficients in
 209 binary mixtures of noble gases with less than 2 % inaccuracy in a broad temperature range (300
 210 to 1400 K), except for Ar-Kr mixtures (33). The same diffusion data, however, are poorly
 211 predicted if σ_{ij} and ϵ_{ij} are calculated with the Lorentz-Berthelot rules (46). The Lennard-Jones
 212 parameters used in the present study are compiled in Table 4.

213 Simulations were carried out with ^4He , ^{20}Ne , ^{40}Ar , ^{84}Kr and ^{132}Xe isotopes to test the quality
214 of the noble gas-water interaction potentials in Table 4, and with a range of hypothetical isotopes
215 of He, Ne, Ar and Xe ($m = 4\text{-}132$ Da) to determine the isotopic mass dependence of solute self-
216 diffusion coefficients. Previous studies have used MD simulation with a broad range of solute
217 mass to infer solute isotopic effects, mainly in Lennard-Jones or hard-sphere fluids (47-49) but
218 also in liquid water (21, 50, 51). Radial distribution functions of O and H atoms near noble gas
219 (NG) solutes and noble gas velocity autocorrelation functions ($\langle \mathbf{v}(0) \cdot \mathbf{v}(t) \rangle$) were calculated with
220 standard methods (41, 52). The average number of oxygen atoms in the first solvation shell of
221 each noble gas (N_{shell}) was calculated by integrating the function $4\pi r^2 g_{\text{NGO}}(r)$ to its first minimum
222 (r_{min}). Solute self-diffusion coefficients were calculated with the well-known Green-Kubo
223 relation (52):

$$224 \quad D = \frac{1}{3} \lim_{\tau \rightarrow \infty} \int_0^{\tau} \langle \mathbf{v}(0) \cdot \mathbf{v}(t) \rangle dt \quad [5]$$

225 The ‘infinite limit’ in equation 5 was approximated accurately by taking the average of D -values
226 obtained for $\tau = 2.4$ to 2.5 ps.

227

228 **Acknowledgments**

229 The research reported in this paper was supported by the Director, Office of Energy
230 Research, Office of Basic Energy Sciences, of the U.S. Department of Energy under Contract
231 No. DE-AC03-76SF00098. This research used resources of the National Energy Research
232 Scientific Computing Center, which is supported by the Office of Science of the U.S.
233 Department of Energy under contract No. DE-AC02-05CH11231. The authors are grateful to DT
234 Bowron and GW Neilson for kindly providing their EXAFS and neutron scattering data.

References

1. Stute M, Forster M, Frischkorn H, Serejo A, Clark JF, Schlosser P, Broecker WS, Bonani G (1995) *Science* 269:379-383
2. Castro MC, Goblet P, Ledoux E, Violette S, de Marsily G (1998) *Water Resour Res* 34:2467-2483.
3. Aeschbach-Hertig W, Peeters F, Beyerle U, Kipfer R (1999) *Water Resour Res* 35:2779-2792.
4. Peeters F, Beyerle U, Aeschbach-Hertig W, Holocher J, Brennwald MS, Kipfer R (2002) *Geochim Cosmochim Acta* 67:587-600.
5. Price RM, Top Z, Happell JD, Swart PK (2003) *Water Resour Res* 39:1267.
6. Zhou Z, Ballentine CJ, Kipfer R, Schoell M, Thibodeaux S (2005) *Geochim Cosmochim Acta* 69:5413-5428.
7. LaBolle EM, Fogg G.E, Eweis JB (2006) *Water Resour Res* 42:W07202.
8. Poreda RJ, Hunt AG, Lyons WB, Welch KA (2004) *Aquat Geochem* 10:353-371.
9. Strassmann KM, Brennwald MS, Peeters F, Kipfer R (2005) *Geochim Cosmochim Acta* 69:1665-1674.
10. Brennwald MP, Kipfer R, Imboden DM (2005) *Earth Planet Sci Lett* 235:31-44.
11. Osenbrück K, Lippmann J, Sonntag J (1998) *Geochim Cosmochim Acta* 62:3041-3045.
12. Rübél AP, Sonntag C, Lippmann J, Pearson FJ, Gautschi A (2002) *Geochim Cosmochim Acta* 66:1311-1321.
13. Hendry MJ, Kotzer TG, Solomon DK (2005) *Geochim Cosmochim Acta* 69:475-483.
14. Higashihara T, Shibuya H, Sato S, Kozaki T (2005) *Eng Geol* 81:365-370.
15. Rodehacke CB, Hellmer HH, Huhn O, Beckmann A (2007) *Ocean Dyn* 57:1-11.

16. Jähne B, Heinz G, Dietrich W (1987) *J Geophys Res* 92:10767-10776.
17. Holz M, Haselmeier R, Mazitov RK, Weingärtner H (1994) *J Am Chem Soc* 116:801-802.
18. Weingärtner H, Haselmeier R, Holz M (1992) *Chem Phys Lett* 195:596-601.
19. Klump S, Tomonaga Y, Kienzler P, Kinzelbach W, Baumann T, Imboden DM, Kipfer R (2007) *Geochim Cosmochim Acta* 71:1385-1397.
20. Richter FM, Mendybaev RA, Christensen JN, Hutcheon ID, Williams RW, Sturchio NC, Beloso AD, Jr (2006) *Geochim Cosmochim Acta* 70:277-289.
21. Bourg IC, Sposito G (2007) *Geochim Cosmochim Acta*, in press.
22. Swope WC, Andersen HC (1984) *J Phys Chem* 88:6548-6556.
23. Straatsma TP, Berendsen HJC, Postma JPM (1986) *J Chem Phys* 85:6720-6727.
24. Tanaka H, Nakanishi K (1991) *J Chem Phys* 95:3719-3727.
25. Guillot B, Guissani Y, Bratos S (1991) *J Chem Phys* 95:3643-3648.
26. Lazaridis T, Paulaitis ME (1994) *J Phys Chem* 98, 635-642.
27. Lau EY, Gerig JT (1995) *J Chem Phys* 103:3341-3349.
28. Arthur JW, Haymet ADJ (1998) *J Chem Phys* 109:7991-8002.
29. Ohmori T, Kimura Y (2005) in *Proceedings of the 14th International Conference on the Properties of Water and Steam*, eds Nakahara M et al (Maruzen Co, Ltd), pp 160-165.
30. Hirschfelder JO, Curtiss CF, Bird RB (1954) *Molecular Theory of Gases and Liquids* (Wiley, New York).
31. Aziz RA (1984) in *Inert Gases: Potentials, Dynamics and Energy Transfer in Doped Crystals*, ed Klein M (Springer, New York), pp 5-86.
32. Tang KT, Toennies JP (1986) *Z Phys D* 1:91-101.
33. Kong CL (1973) *J Chem Phys* 59:2464-2467.

34. Broadbent RD, Neilson GW (1994) *J Chem Phys* 100:7543-7547.
35. Bowron DT, Filipponi A, Lobban C, Finney JL (1998) *Chem Phys Lett* 293:33-37.
36. Geiger A, Rahman A, Stillinger FH (1979) *J Chem Phys* 70:263-276.
37. Rapaport DC, Scheraga HA (1982) *J Phys Chem* 86:873-880.
38. Kirchner B, Stubbs J, Marx D (2002) *Phys Rev Lett* 89:215901.
39. Filipponi A, Bowron DT, Lobban C, Finney JL (1997) *Phys Rev Lett* 79:1293-1296.
40. Bowron DT, Weigel R, Filipponi A, Roberts MA, Finney JL (2001) *Mol Phys* 99:761-765.
41. Refson K (2000) *Comput Phys Commun* 126:310-329.
42. Berendsen HJC, Grigera JR, Straatsma TP (1987) *J Phys Chem* 91:6269-6271.
43. Smith DE, Dang LX (1994) *J Chem Phys* 100:3757-3766.
44. Wasserman E, Wood B, Brodholt J (1995) *Geochim Cosmochim Acta* 70:277-289.
45. Hura G, Russo D, Gleaser RM, Head-Gordon T, Krack M, Parrinello M (2003) *Phys Chem Chem Phys* 5:1981-1991.
46. Hogervorst W (1971) *Physica* 51:77-89.
47. Alder BJ, Alley WE, Dymond JH (1974) *J Chem Phys* 61:1415-1420.
48. Nuevo MJ, Morales JJ, Heyes DM (1995) *Phys Rev E* 51:2026-2032.
49. Willeke M (2003) *Mol Phys* 101:1123-1130.
50. Wilson MA, Pohorille A, Pratt LR (1985) *J Chem Phys* 83:5832-5836.
51. Møller KB, Rey R, Masia M, Hynes JT (2005) *J Chem Phys* 122:114508.
52. Allen MP, Tildesley DJ (1987) *Computer Simulation of Liquids* (Clarendon Press, Oxford).

Table 1. Self-diffusion coefficients ($10^{-9} \text{ m}^2 \text{ s}^{-1}$) of noble gases in ambient liquid water.

Noble gas	Experimental (16)	Experimental (17, 18)	MD simulation (29)	MD simulation (this study)
He	7.22 ± 0.36		10.0 ± 0.9	7.85 ± 0.54
Ne	4.16 ± 0.21	4.18 ± 0.20	4.9 ± 0.2	4.78 ± 0.37
Ar			2.4 ± 0.1	2.57 ± 0.15
Kr	1.84 ± 0.09		2.1 ± 0.1	1.97 ± 0.13
Xe	1.47 ± 0.07	1.90 ± 0.09^a	1.6 ± 0.1	1.57 ± 0.11

^a confidence interval calculated with the assumption that NMR data for Ne and Xe diffusion have similar coefficients of variation.

Table 2. Location of the first maximum and minimum of $g_{NGO}(r)$ and first-shell coordination number of O atoms around noble gas solutes in ambient liquid water. Confidence intervals on r_{\max} and r_{\min} values are ± 0.05 Å.

Noble gas	r_{\max} (Å)	r_{\min} (Å)	N_{shell}
He	3.0	4.7	14.0 ± 0.4
Ne	3.1	4.9	15.7 ± 0.4
Ar	3.5	5.2	18.8 ± 0.5
Kr	3.7	5.4	21.2 ± 0.5
Xe	3.9	5.6	22.4 ± 0.5

Table 3. Parameters of the linear regression equation $\log(D) = A - \beta \cdot \log(m)$ calculated with 16 paired D, m values for each noble gas solute.

Solute	A	β	R^2
He	1.00 ± 0.04	0.171 ± 0.028	0.91
Ne	0.87 ± 0.03	0.150 ± 0.018	0.95
Ar	0.52 ± 0.04	0.078 ± 0.024	0.75
Xe	0.33 ± 0.03	0.059 ± 0.023	0.65

Table 4. Lennard-Jones 6-12 potential parameters.

Atom pair	σ (Å)	ϵ (kJ mol ⁻¹)
<i>Noble gas-water interaction</i>		
He-O	2.9730	0.20500
Ne-O	2.9758	0.45416
Ar-O	3.2645	0.86608
Kr-O	3.3948	0.98380
Xe-O	3.5874	1.07990
<i>Water-water interaction (42)</i>		
O-O	3.1656	0.65017

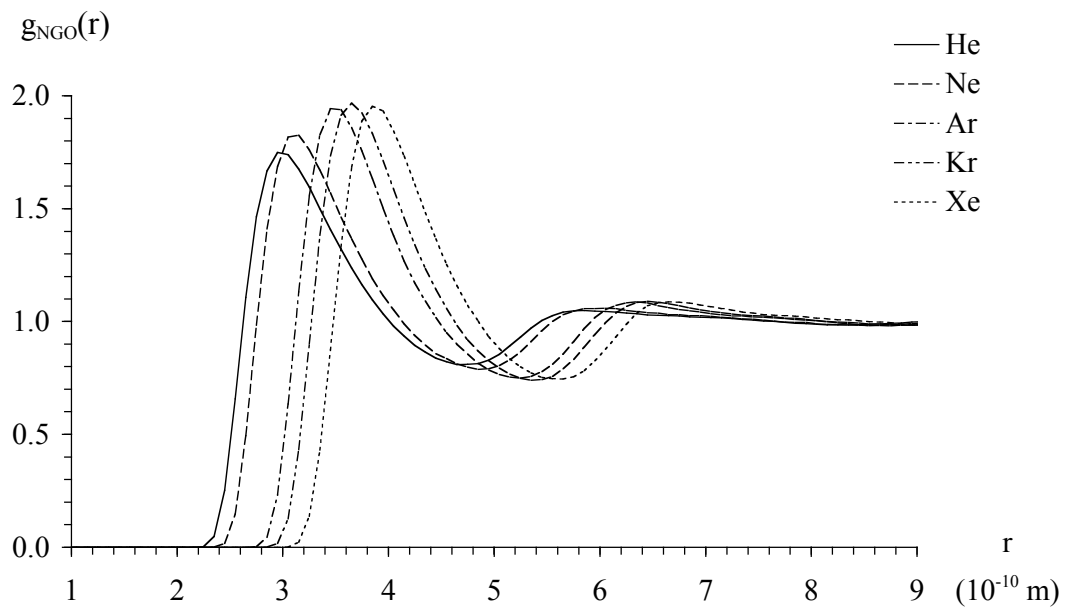
List of Figures

Fig. 1. Radial distribution functions of (a) O atoms and (b) H atoms near noble gases in liquid water at 298 K.

Fig. 2. Snapshot of a ^{40}Ar atom (in green) and water molecules located in its first solvation shell (i.e., at Ar-O distances $< 5.2 \text{ \AA}$). Highlighted water molecules in the upper and lower parts of the figure illustrate the two possible ‘straddling’ configurations, with either a lone pair of electrons (upper part of the figure) or an H atom (lower part of the figure) pointing away from the solute.

Fig. 3. Experimental and simulated self-diffusion coefficients of noble gases in liquid water at 298 K, plotted as a function of solute radius.

a)



b)

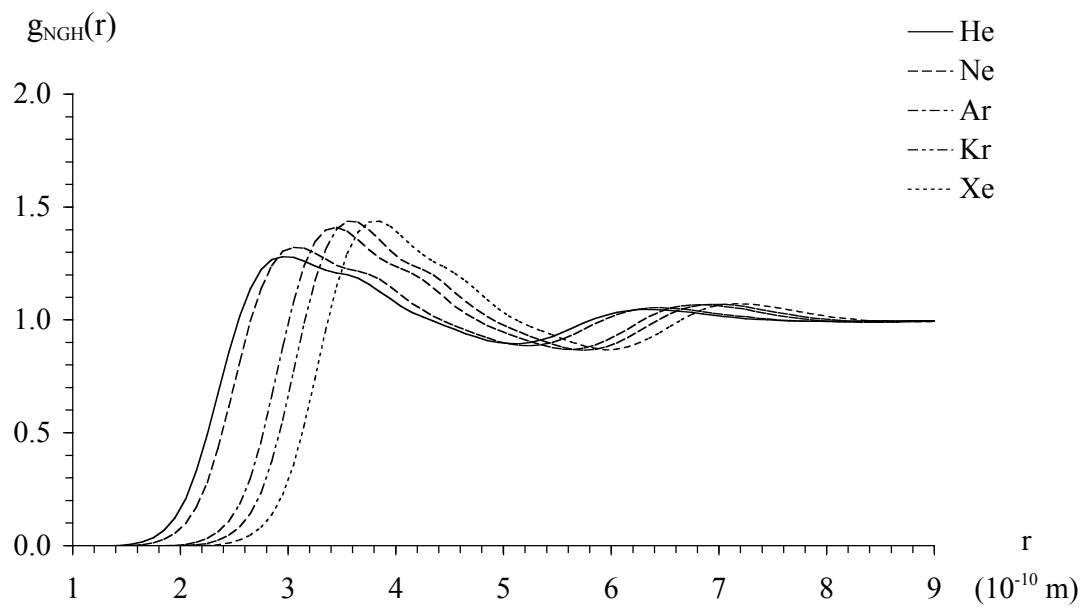


Figure 1.

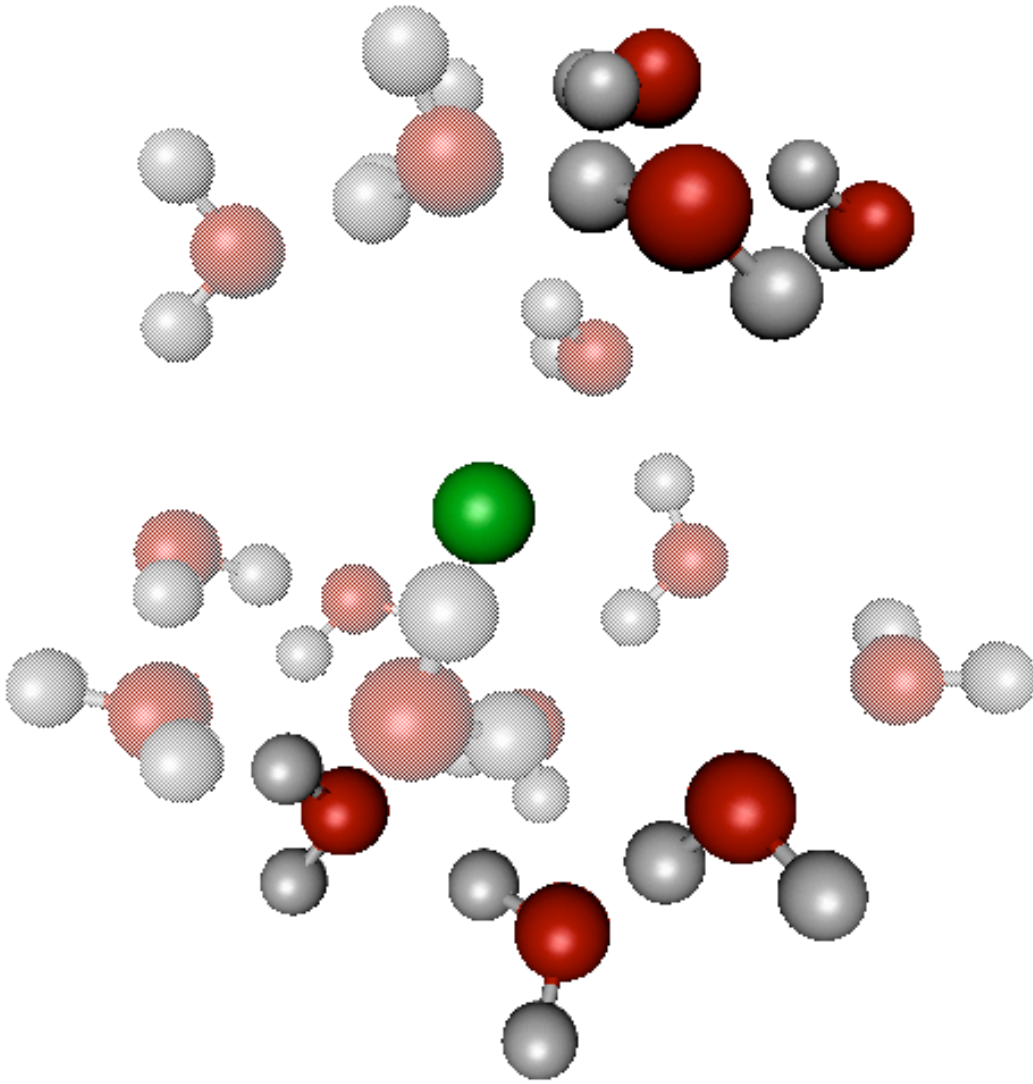


Figure 2.

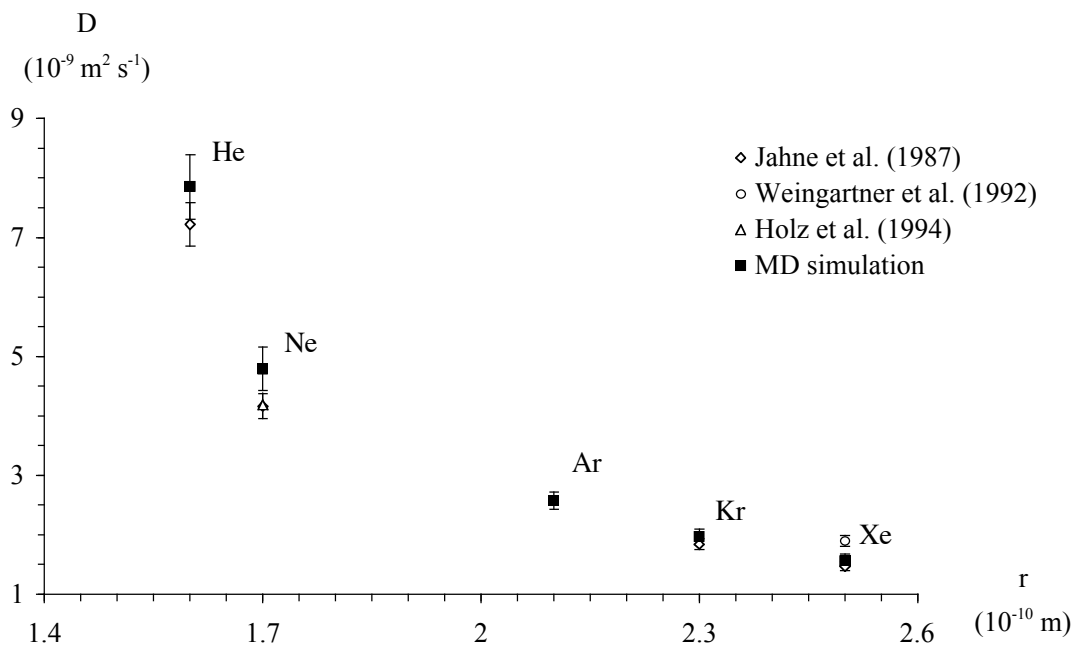


Figure 3.